Carpathian Journal of Earth and Environmental Sciences, November 2012, Vol. 7, No. 4, p. 47 - 60

APATITE AS A PETROGENETIC INDICATOR OF VARISCAN GRANITOIDS IN TISZA MEGA-UNIT (SOUTH HUNGARY)

György BUDA[1] & Elemér PÁL-MOLNÁR[2]

[1]Department of Mineralogy, Eötvös Loránd University, H-1117 Budapest, Pázmány P. str. 1/C, Hungary, (buda@ludens.elte.hu)

[2]Department of Mineralogy, Geochemistry and Petrology, University of Szeged, H-6701 Szeged, P.O. Box 651, Hungary (palm@geo.u-szeged.hu)

Abstract: Apatite is an excellent indicator of the origin of granitoid rocks. Two types of granitoids occur in Tisza Mega-Unit, south Hungary: one is in Kunságia (Mórágy Subunit); the other is in Békésia Unit (Battonya Subunit). Both granitoids contain apatite as accessory mineral. Apatite in metaluminous granitoids of Mórágy Subunit is characterized by REE- (Ce enriched) and chlorine-bearing fluorapatite, depleted in Mn, and is zoned, acicular, or prismatic with rather small grain sizes that are almost inclusion-free. In Battonya Subunit apatite is found in basic quartz monzodiorite and it is acicular and Mn-free; in the peraluminous granitoids it is Mn-rich, low REE-bearing, chlorine-poor, and unzoned, containing monazite and zircon inclusions, with stubby habit and large grain sizes. The two contrasting chemistries, textures, and crystal habits of apatite are due to the different origins of the granitoid melts. In Mórágy Subunit the I-type granitoids crystallized at higher temperature and therefore the oxidized Mn^{3+} could not enter in the apatite structure, and due to the low Al-content of the melt, REEs entered the allanite and apatite, whereas in the majority of Battonya Subunit the S-type granitoid melt had a lower temperature and consequently Mn^{2+} entered the apatite structure, substituting for Ca^{2+}, and at first monazite crystallized from the peraluminous melt, consuming REEs from the melt, causing depletion in the REEs of apatite, and the sedimentary origin probably caused chlorine depletion.

Keywords: granitoids, apatite, I-type, S-type, Variscan, Mórágy Subunit, Battonya Subunit, Hungary

1. INTRODUCTION

Apatite occurs as an accessory mineral in nearly every magmatic rock from basic to acidic and is a sensitive recorder of the trace element chemistry of magmatic systems (Ayers & Watson, 1993; Belousova et al., 2001; Piccoli & Candela, 2002; Hoshino et al., 2007; Marks et al., 2012). The primary aim of this study is to use the apatite as an indicator of the genesis of granitoids. The composition of granitic magma depends on the source rocks but can be changed by fractional crystallization, hydrothermal alteration, and so on. Granitic source rock can be of magmatic (I-type) or sedimentary (S-type) origin, showing significant differences in chemical, isotopic, and mineralogical compositions. The chemical composition of minerals is a function of temperature, pressure, fugacity, activity, and coexisting phases. In the I- and S-type granitic rocks, apatites have different habits, textures, and chemical characters.

The chemical composition was analyzed by microprobe, and back-scattered electron images were used to reveal the element distributions, textures, and inclusions in the crystals in order to obtain an idea of the origin of the host granitic rock. The studied rocks were Variscan granitoids of Tisza Mega-Unit (TMU, Hungary), where I- as well as S-type granitoids occur.

2. GEOLOGICAL SETTING

The TMU comprises the crystalline basement of south Hungary, east Croatia, north Serbia, and the western part of Transylvania (Romania) (Kovács et al., 2000; Haas, 2001). It is bordered by the Mid-Hungarian Lineament, the Száva-Moslavima-Zombor-Bečej-Lipova line (the northern border of the Srem–Mureş Ophiolite Belt), and the Someş Lineament in the northwest, south, and northeast,

respectively. The basement is covered by thick Miocene–Pliocene sediments. During the Neogene the Pannonian Basin has undergone a complex tectonic evolution that has principally modified the original Variscan structures of the area (Tari et al., 1999; Csontos & Nagymarosi, 1999). As an independent unit the TMU existed from the Late Cretaceous, when its rotation began, until the Early Miocene (Csontos, 1995; Márton, 2000, 2001; Kovács et al., 2000). Separation from the Moldanubian Zone of Variscan Europe started in the Late Triassic–Early Cretaceous, recorded by crystalline rocks and sedimentary sequences (Haas & Péró, 2004; Csontos & Vörös, 2004; Schmid et al., 2008).

The Hungarian part of the TMU, where Variscan granitoids were identified, is called the Kunságia Unit (KU) and Békésia Unit (BU) (Haas, 2001) (Fig. 1). The BU can be divided into four subunits: Kelebia, Csongrád, Battonya, and Sarkadkeresztúr. The Battonya Subunit is a 15–25 km long, 10–15 km wide body forming a flat anticline covered by 1000–1500 m thick Miocene and Pannonian sediments (Fig. 1B). The majority of the KU is also covered by sediments, and it outcrops on the surface only in the eastern part of Mecsek Mts. in the Mórágy Subunit (Fig. 1C).

Two main types of Variscan granitoids were identified in these units. Both have similar ages of about 340–360 Ma (U/Pb, K/Ar, Sr/Rb) (Kovács et al., 2000).

3. SAMPLING AND ANALYTICAL METHODS

The samples from Mórágy Subunit were collected from outcrops, boreholes, and tunnels. The samples from Battonya Subunit were obtained from the boreholes around Battonya, Mezőhegyes, Pitvaros, and Kunágota settlements. The rocks were acquired from the rock collection of the Department of Mineralogy, Geochemistry, and Petrology, University of Szeged. The samples are drill-cores and consequently their numbers are limited.

The major element analyses of the rocks were carried out by the ICP-AES method (lower detection limit for major components: 0.01 wt%); FeO content was determined by titrimetric and H_2O^- and H_2O^+ by gravimetric methods; ICP-MS was used for trace element analyses (lower detection limits were 0.5 or 0.03 ppm). Analyses were executed by ALS Chemex in Canada (Vancouver). The 70 quantitative analyses of apatite were carried out with a CAMECA SX100 electron microprobe using WDS, at the Institute of Geological Sciences, Masaryk University, Brno, Czech Republic, on polished and carbon coated thin sections. Analytical conditions for apatite were as follows: an accelerating voltage of 15 kV and

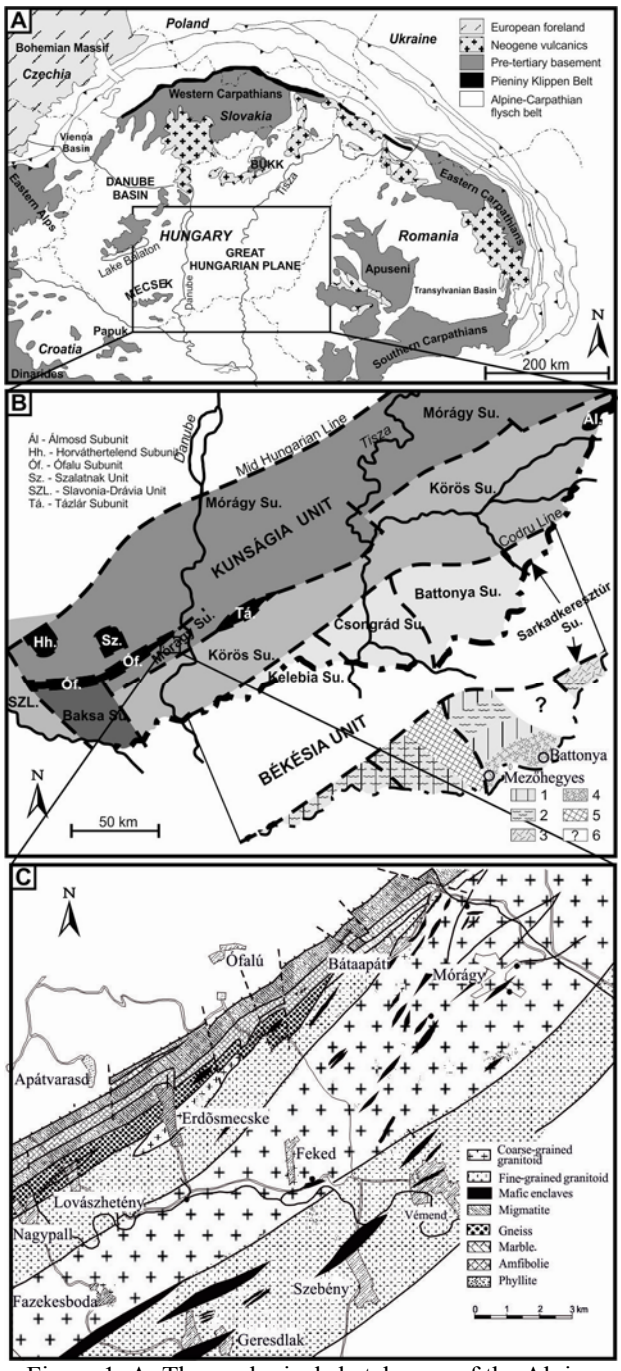

Figure 1. A. The geological sketch map of the Alpine-Carpathian-Pannonian region; B**.** Pre-Tertiary regional geological map of the Tisza Mega-Unit (SE part of the Pannonian Basin) showing the Variscan granitoids (modified after Kovács et al., 2000) – 1. Alpine overstep sequence connected to the northern shelf of the Axios/Vardar and related Neotethyan oceanic basins; 2. Variscan medium-grade metamorphosed complex; 3. Migmatitic complex; 4. Granitoids; 5. Dorozsma Complex; Permian overprinted by Cretaceous amphibolite facies (Lelkes et al., 2003); 6. Unknown; C. Geological map of Mórágy Subunit

electron beam current of 20 nA for Ca, P, F, Na, and Mn, and an accelerating voltage of 15 kV and electron beam current 40 nA for other elements. The electron beam was defocused to 4 μm. The following standards were used: for Na, albite; for Si, and Fe, almandine; for Al, and K, sanidine; for Mg, Mg_2SiO_4; for La, LaB; for Ce, CeAl; for U, U; for Sc, $ScVO_4$; and for P, fluorapatite. Modified standards were used as follows: for Ca, grossular; for Ti, titanite; for Mn, spessartine, for Nd, $NdPO_4$; for Sm, SmF_3; for Pr, PrF_3; for Dy, $DyPO_4$; for Er, $ErPO_4$; for Gd, $GdPO_4$; for Th, Th; for F, topaz, and so on. Peak counting times were 10 seconds for major elements and 40 to 60 seconds for minor to trace elements. Matrix corrections were performed using the PaP software routine.

4. CHARACTER OF HOST GRANITOIDS

4.1. Mórágy Subunit (Mórágy Complex)

These granitoids are magnesio-potassic, met/peraluminous (ASI ≈ 1.00 ± 0.04, A/NK≈1.56 ± 0.10, n=20), microcline megacryst-bearing amphibole-biotite quartz monzonite and monzogranite (Fig. 2A, B, Tab. 1) with several highly potassic, metaluminous (ASI≈0.77±0.13, A/NK≈1.53±0.13, n=23) mafic enclaves (melamonzonite, melasyenite, locally named vaugnerite/durbachite), transected by slightly peraluminous microgranite dikes (ASI≈1.05±0.07, A/NK≈1.26, n=6). At the border of the granitoid and the enclave, so-called hybrid rock (melamonzonite) occurs with a high content of microcline and amphibole (ASI=0.91, A/NK=1.49) and very high ΣREE (800 ppm) as a result of enrichment with allanite, and it is consequently LREE enriched (La_N/Yb_N=45) with a negative Eu anomaly (Eu/Eu^*=0.47).

In the main granitoid body, microcline (Δ=0.9) occurs as megacrysts and forms small crystals in the groundmass (Δ=0.5) of white and pinkish colour. Plagioclases are mostly zoned; sometimes a "spike" zonation can be observed (An_{35-45}, spike: An_{60}), and quartz forms knots with mostly undulatory extinction. Actinolite and Mg-hornblende are common. The hornblende and biotite in granitoids are richer in Fe ($(Fe/(Fe+Mg)_{bi}$=0.48, 0.37_{horn}) than those in enclaves (0.40_{bi}, $0.29_{horn.}$). In enclaves amphibole forms "pilites" with tiny chromite grains or forms as a uralitization product of ferrodiopside (Buda & Dobosi, 2004).

The whole intrusive body belongs to calc-alkaline K-rich monzonitic series. It is K, Mg, and Ca enriched whereas Al and Si contents are comparatively low ($D_{gran.}$ = Na + K + 2Ca/Al (Si+Al)=1.19±0.06, D_{encl}=1.74±0.27; Montel, 1993). Due to the high Ca activity, besides apatite and titanite, a high amount of allanite crystallized in the enclaves as well as in the enclosing granitoids (Buda et al., 2010). Allanite is the major REE-rich mineral which controls the whole-rock REE patterns ($\Sigma REE_{encl.}$≈450 ppm, Eu/Eu*≈0.60 La_N/Yb_N=20, $\Sigma REE_{gran.}$≈270 ppm, Eu/Eu*≈0.75, La_N/Yb_N=30, Fig. 2C, Table 1)

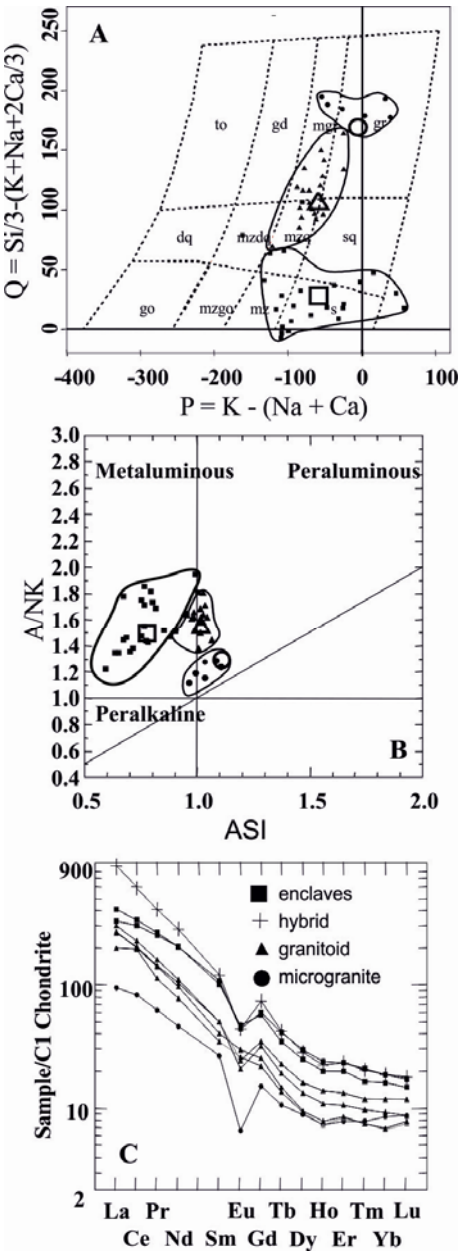

Figure 2. A. Classification of granitoids from Mórágy Subunit: □=average of enclaves (syenite, monzonite), Δ =average of granitoids (q-monzonite, monzogranite), ○=average of microgranites (Debon & Le Fort, 1983); B. Alumina-saturation of granitoids (Mórágy Subunit); C. Chondrite normalised REE distribution of granitoids (Mórágy Subunit)

Table 1. Representative chemical composition of enclaves, hybrid rocks, granitods and microgranite from Mórágy Subunit

wt%	Enclaves		Hybrid rock	White microcline-bearing granitoid		Pinkish microcline-bearing granitoid		Microgranite
	1	2	3	4	5	6	7	8
SiO_2	53.60	52.30	53.70	65.00	60.10	61.80	69.00	76.30
TiO_2	1.51	1.55	1.47	0.77	0.80	0.52	0.51	0.08
Al_2O_3	14.65	15.05	16.65	15.10	16.75	16.40	14.35	12.40
Fe_2O_3	2.13	2.02	2.16	0.97	1.48	1.36	0.90	0.28
FeO	5.13	4.89	4.50	3.37	3.07	0.37	2.12	0.25
MnO	0.12	0.09	0.09	0.06	0.06	0.05	0.04	0.01
MgO	5.93	6.10	5.82	2.36	3.23	1.68	1.74	0.09
CaO	5.29	5.41	3.96	3.27	4.09	3.86	1.81	0.84
Na_2O	2.28	2.35	3.57	3.19	4.09	3.71	2.93	2.68
K_2O	6.74	6.66	4.88	3.95	3.94	4.83	4.85	6.30
P_2O_5	0.90	0.88	0.59	0.26	0.35	0.20	0.16	0.01
H_2Op	0.20	0.22	0.21	0.13	0.22	0.37	0.13	0.27
H_2Om	1.05	1.84	2.27	0.77	1.48	4.04	1.85	1.13
Total	99.53	99.36	99.87	99.20	99.66	99.19	100.39	100.64
ASI	0.71	0.72	0.91	0.98	0.91	0.89	1.07	0.97
Ba	2190.00	2390.00	1115.00	903.00	975.00	1025.00	818.00	175.50
Rb	259.00	261.00	356.00	183.50	218.00	248.00	182.50	244.00
Sr	850.00	900.00	805.00	386.00	796.00	648.00	310.00	83.10
Cs	7.82	6.77	12.40	9.61	6.21	5.07	10.30	8.14
Ga	22.30	23.20	29.10	21.80	24.40	22.40	19.50	15.70
Tl	0.90	0.80	1.30	0.80	0.90	1.20	0.80	0.90
Ta	3.90	3.50	3.80	2.20	1.00	1.30	2.10	3.10
Nb	36.20	36.50	32.70	18.90	14.50	16.30	16.00	8.20
Hf	13.40	13.10	14.40	8.60	9.10	6.00	7.00	4.10
Zr	460.00	474.00	508.00	306.00	330.00	213.00	231.00	80.00
Ti	905.00	929.00	881.00	462.00	480.00	312.00	0.00	48.00
Y	36.50	30.30	34.10	20.90	12.00	11.80	15.70	10.40
Th	35.20	39.40	57.30	31.80	21.60	32.60	53.90	39.70
U	8.44	8.58	12.55	7.91	8.58	3.01	12.55	3.51
Cr	240.00	250.00	230.00	60.00	90.00	70.00	40.00	10.00
Ni	158.00	161.00	71.00	20.00	31.00	22.00	13.00	5.00
Co	33.20	32.60	33.70	21.40	21.10	16.40	19.70	31.60
V	120.00	123.00	123.00	68.00	76.00	51.00	43.00	5.00
Cu	31.00	36.00	42.00	11.00	26.00	18.00	5.00	15.00
Pb	35.00	36.00	29.00	38.00	32.00	36.00	45.00	45.00
Zn	106.00	97.00	99.00	71.00	64.00	54.00	55.00	11.00
Sn	10.00	10.00	11.00	4.00	3.00	4.00	3.00	4.00
W	84.00	69.00	92.00	211.00	169.00	173.00	247.00	549.00
Mo	2.00	2.00	2.00	2.00	2.00	2.00	2.00	2.00
C	0.03	0.05	0.09	0.03	0.04	0.55	0.05	0.11
Ag	1.00	1.00	1.00	1.00	1.00	1.00	1.00	1.00
Hg	0.07	0.08	0.10	0.22	0.09	0.14	0.25	0.43
S	0.08	0.08	0.08	0.03	0.07	0.01	0.01	0.01
As	0.90	1.30	2.70	3.60	3.10	1.00	2.60	5.50
Se	0.20	0.20	0.20	0.20	0.30	0.20	0.20	0.20
Sb	0.11	0.06	0.06	0.06	0.17	0.22	0.06	0.12
Te	0.01	0.01	0.01	0.01	0.01	0.01	0.01	0.01
La	78.20	96.30	211.00	62.10	64.40	47.10	71.50	22.20

Table 1. (continue)

ppm	Enclaves		Hybrid rock	White microcline-bearing granitoid		Pinkish microcline-bearing granitoid		Microgranite
	1	2	3	4	5	6	7	8
Ce	184.00	205.00	370.00	123.00	122.00	119.00	139.50	51.20
Pr	24.20	25.30	39.20	13.70	13.20	10.65	15.30	5.87
Nd	95.80	95.50	130.50	48.10	44.60	35.90	51.20	21.20
Sm	16.35	15.35	18.45	7.70	6.15	5.24	7.70	4.04
Eu	2.56	2.74	2.56	1.42	1.70	1.52	1.22	0.38
Gd	12.25	11.85	15.15	7.08	5.21	4.47	6.46	3.08
Tb	1.53	1.30	1.57	0.86	0.55	0.50	0.71	0.40
Dy	7.49	6.35	7.13	4.12	2.42	2.38	3.34	2.24
Ho	1.36	1.12	1.26	0.78	0.44	0.41	0.61	0.41
Er	3.88	3.34	3.85	2.18	1.40	1.37	1.75	1.28
Tm	0.53	0.42	0.52	0.30	0.19	0.19	0.25	0.20
Yb	3.19	2.73	3.19	2.01	1.15	1.14	1.57	1.45
Lu	0.44	0.37	0.45	0.30	0.20	0.19	0.22	0.22
∑REE	431.78	467.67	804.83	273.65	263.61	230.06	301.33	114.17
Eu/Eu*	0.55	0.62	0.47	0.59	0.92	0.96	0.53	0.33
La_N/Yb_N	16.53	23.78	44.59	20.83	37.75	27.85	30.70	10.32

1. Amphibole-biotite (large, flacky)-rich, white plagioclase, pinkish microcline-bearing enclave (6.s.); 2. Amphibole-biotite-rich enclaves very similar to the sample No.6.(7 s.); 3. Amphibole-biotite-rich hybrid rock with pinkish microcline (12a.s.); 4. White microcline-bearing granitoid (13 s.); 5. White microcline-bearing granitoid (27a s.); 6. Pinkish microcline-bearing granitoid with carbonate veins (17.a s.); 7. Pinkish microcline megacrystal-bearing granitoid; 8. Pinkish fine-grained aplitic granite (KA484 s.) (s=sample)

Allanites are oxidized ($Fe^{3+}/Fe^{tot}\approx0.4$), as is characteristic of the igneous allanite in the I-type granitoids (Broska et al., 2000). Altered allanites are enriched in ΣREE and depleted in Al and Ca. In microgranite, allanite was not identified (D=1.09±0.06), the ΣREE content is low (110 ppm), the negative Eu anomaly (Eu/Eu*≈0.33) is large, and the REE chondrite normalized distribution is flat, and consequently the ΣLREE/ΣHREE ratio is the lowest among the three rock types (La_N/Yb_N=10).

The basic (enclaves) and acidic (granitoids) melts probably crystallized at the same time. The basic melt originated from the upper mantle, and the acidic melt formed by partial melting of the continental crust (Buda et al., 2004a). Apatite occurs in granitoids as well as in enclaves.

4.2. Battonya Subunit (Battonya Complex)

These granitoids have a slight thermal contact zone and are surrounded by regional metamorphic rocks and partly covered by Alpine sequences. Generally they are medium-grained equigranular, sometimes with pinkish microcline megacrysts. The majority contain biotite and/or muscovite. Three rock types have been distinguished:

I. Quartz monzodiorite (Fig. 3) is the greenish grey variety containing amphibole-biotite without primary muscovite. It is mostly metaluminous (ASI=0.8, Fig. 3B, Tab. 2). Amphiboles form large eu- and sub-hedral crystals or small aggregates. The large amphibole is zoned; the core is Mg-hornblende with low Si and high Al, Ti, and Cr contents and the rim is actinolite. Biotite is subhedral, Mg-rich (Fe/(Fe+Mg)=0.31), and Al poor with a phlogopitic composition having a calc-alkaline (Abdel-Rahman, 1994; Buda et al., 2004b) character. Sometimes it occurs in the form of anhedral patches in amphibole showing replacement texture. Alteration of biotite to chlorite is common. Primary muscovite is missing but the secondary one (sericite) is common in plagioclase. The plagioclases have oscillatory zoning between oligoclase (An_{17-13}) and andesine (An_{43-40}) with secondary albitization and sericitization. Sometimes they are unzoned oligoclases (An_{17-10}). Cross-hatched microcline is not common; it shows replacement texture without perthitic exsolution, with low Na content in the structure. Quartz is rare, and is deformed with wavy extinction. Secondary calcite can be observed. Accessory minerals are acicular apatite, zircon, and very rarely monazite. This rock has high ΣREE (≈250 ppm, La_N/Yb_N=19) and a very low negative Eu-anomaly (Eu/Eu*=0.91; Fig. 3C).

II. and III. Granodiorite-granite: These granitoids are the most common in the intrusion. Differences between the granodiorite and granite are not well defined because of the different rates of alteration, which can screen the primary rock

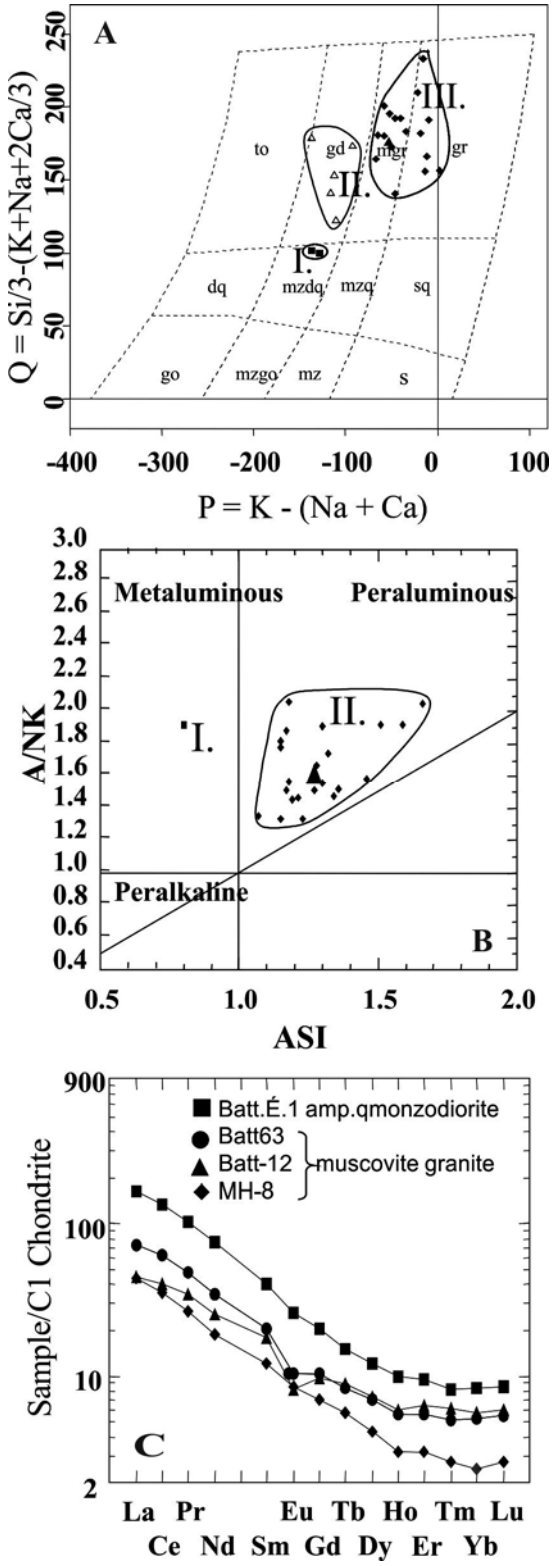

Figure 3. A. Classification of granitoids from Battonya Subunit I. – quart monzodiorite, II. – granodiorite, III. – monzogranite, granite; B. Alumina-saturation of granitoids (Battonya Subunit) ; C. Chondrite normalised REE distribution of granitoids (Battonya Subunit)

chemical and mineral composition, for example the K-feldspar/plagioclase ratio. Granodiorite-granite is grey with biotite and muscovite or only muscovite and sometimes contains microcline megacrysts.

These rocks are strongly peraluminous ($ASI_{avg.}$=1.3, CIPW $corundum_{average}$=4). Biotite is Fe-rich (Fe/(Fe+Mg)=0.58) and strongly pleochroic, with peraluminous (Pál-Molnár et al., 2001; Buda et al., 2004b) chemical characters, sometimes entirely altered to chlorite. Euhedral or subhedral large primary muscovite is common. Sometimes it has grown across the biotite, indicating later crystallization from Al-rich water-saturated melt. The plagioclase is sometimes oscillatory zoned. The cores are mostly oligoclase (An_{25-10}) and the rims are albite (An_{10-0}). The cores are strongly sericitized or altered to clay minerals, partly replaced by crossed-hatched microcline and albite. Albite and microcline with low Na (Or_{97}) content are widespread, occurring in replacement textures. Maximum or nearly maximum microcline (Δ=0.74; Buda, 1975) occurs as megacrysts without perthitic exsolution. Quartz is ubiquitous with wavy extinction; it occurs rarely as myrmekite in plagioclase. Stubby apatite, zircon, and monazite are common as accessory minerals. The REE minerals are monazite (D_{rock} = 0.9) and tiny grains of xenotime which crystallized before apatite. Muscovite granite has low ΣREE content (90 ppm, (Table 2, Fig. 3/C) with strongly variable Eu anomalies (Eu/Eu*=0.62–0.93).

The REE pattern is controlled by zoned monazite. The core of monazite is slightly richer in HREEs than the outer zone (Buda et al., 2009).

The majority of the Battonya granitoids are two-mica granodiorite and granite and are peraluminous (ASI>1). The amphibole-bearing quartz monzodiorite is metaluminous I-type and the muscovite-rich granitoid is S-type, belonging to the calc-alkaline granodioritic-series. Granitoid formed from melting of "wet" crustal rocks where two continental lithospheres underplated after the collision.

5. APATITE TEXTURE AND CHEMISTRY

Apatites show significant differences in the two types of granitoids with respect to the crystal chemistry as well as textures, habits, inclusions, and so on. In the same unit the apatite shows differences in several respects in different rock types.

5.1. Mórágy Subunit

Apatite occurs in every rock type, but the textures and compositions are different.

Enclaves (melamonzonite, melasyenite): Apatites occur in titanite, amphibole, and biotite, sometimes forming acicular crystals.

Table 2. Representative chemical composition of granitoids from Battonya Subunit

wt%	Amp. Q-monzodiorite	Muscovite granite		
	1.	2.	3.	4.
SiO_2	55.30	71.90	72.60	73.30
TiO_2	0.66	0.24	0.26	0.12
Al_2O_3	13.85	14.80	14.65	13.90
Fe_2O_3	1.58	0.26	0.37	0.25
FeO	4.11	0.25	0.32	0.57
MnO	0.14	0.02	0.01	0.01
MgO	7.63	0.24	0.36	0.30
CaO	5.50	1.26	0.40	0.92
Na_2O	2.66	3.81	3.04	3.06
K_2O	2.62	3.79	3.94	5.00
P_2O_5	0.32	0.16	0.26	0.06
H_2Op	2.87	1.34	1.84	0.54
H_2Om	0.18	0.08	0.11	0.07
CO_2	0.75	0.95	0.05	1.06
Total	98.17	99.10	98.21	99.16
ASI	0.80	1.17	1.47	1.15
Ba	612.00	607.00	631.00	999.0
Rb	166.00	154.50	199.00	115.0
Sr	705.00	261.00	170.50	265.0
Y	21.00	12.40	13.80	7.60
Zr	159.0	106.00	94.00	52.00
Nb	16.60	11.50	13.80	4.30
Th	12.00	8.20	8.64	5.28
Ga	18.70	20.40	20.50	15.10
Cu	–	–	10.00	–
V	127.00	22.00	21.00	10.00
Cr	420.00	10.00		10.00
Hf	4.10	3.10	3.20	1.70
Cs	13.80	3.17	5.20	2.70
Ta	1.10	2.40	4.00	1.50
U	3.31	3.23	4.79	1.35
W	82.00	285.00	780.00	468.0
Sn	2.00	3.00	4.00	3.00
La	51.80	23.30	14.40	14.00
Ce	109.00	50.90	33.30	28.70
Pr	12.45	5.75	4.20	3.19
Nd	47.10	21.30	15.60	11.60
Sm	8.03	4.11	3.58	2.42
Eu	1.98	0.78	0.62	0.65
Gd	5.47	2.79	2.58	1.87
Tb	0.74	0.41	0.44	0.28
Dy	3.99	2.30	2.42	1.41
Ho	0.75	0.42	0.45	0.24
Er	2.07	1.20	1.37	0.69
Tm	0.27	0.17	0.20	0.09
Yb	1.86	1.17	1.28	0.54
Lu	0.28	0.18	0.20	0.09
∑ REE	245.79	114.78	80.64	65.77
Eu/Eu*	0.91	0.70	0.62	0.93
La_N/Yb_N	18.78	13.43	7.58	17.48

Two different Mn contents can be distinguished: (a) apatite with a detectable amount of Mn; (b) apatite with Mn-content under the detection limit (Table 3). The Fe content is strongly variable. These apatites are zoned; the outer zone is enriched in La, Ce, and Nd ($\Sigma REE_{average}$≈4700 ppm, La≈1300 ppm, Ce≈2400 ppm, Nd≈850 ppm). The F content is 2.96 wt%, and the Cl content is 0.03 wt% (Fig. 4/1–4).

Hybrid rock (monzonite): Irregular distribution of REEs can be observed in one crystal of apatite. It shows a "whirlpool" texture (Fig. 4/5). Average ΣREE≈7300 ppm (La≈1900 ppm, Ce≈4100 ppm, Nd≈1000 ppm, F=2.99 wt%, Cl=0.07 wt%).

Q-monzonite-monzogranite (granitoids): Two varieties of apatite were distinguished in these rocks also: (a) Mn-free or poor and (b) Mn-bearing (Table 3, Fig. 5). The zoned crystals are common. The outer zone is enriched in LREEs (Fig. 4/6, 8; Fig. 6/1). Average ΣREE≈3900 ppm (La≈400 ppm, Ce≈1500 ppm, Nd≈1300 ppm). Sometimes it contains thorite inclusions where Y and Th enrichment of the apatite also occurs (Fig. 4/7; F=3.23 wt%; Cl=0.01 wt%).

5.1.1. Summary

Apatite is depleted in Mn in all rock types (Fig. 5/A) which is a characteristic of I-type granitoids (Broska et al., 2002) and is enriched in LREEs, especially in Ce and Nd. Chlorine content is also detectable, mostly in enclaves and hybrid rocks. Zonation is common, with LREE enrichment occurring at the rims of crystals. Inclusions are rare.

Fluorine content increases and chlorine decreases from enclaves to granitoids. Average grain sizes are 130 μm.

5.2. Battonya Subunit

Apatite occurs in every rock type, showing different morphologies and compositions.

Amphibole quartz monzodiorite: Apatite is always acicular (Fig. 6/2). It occurs in every rock-forming mineral (amphibole, biotite, plagioclase, quartz). Apatite is inclusion free, without zonation. Mn and REE contents are very, low but Fe-content is significant (FeO=0.1 wt%). Fluorine content is 3.05 wt%.

Two-mica granodiorite and granite: Apatite is euhedral and forms well developed stubby crystals (Fig. 6/3 and 4) without zonation and inclusions. Apatite occurs in biotite and muscovite as well as in altered plagioclase. Apatite contains manganese (MnO=0.16 wt %) and has low Fe-content (Table 4, Fig. 5/B). Y, Ce, Nd, and Dy content can be detected (ΣREE≈1500 ppm). Fluorine content is higher compared with the apatite occurring in quartzmonzodiorite (F=3.43 wt%).

Muscovite granite: Apatite is euhedral and stubby (Fig. 6/5, 6). It is not zoned but contains small

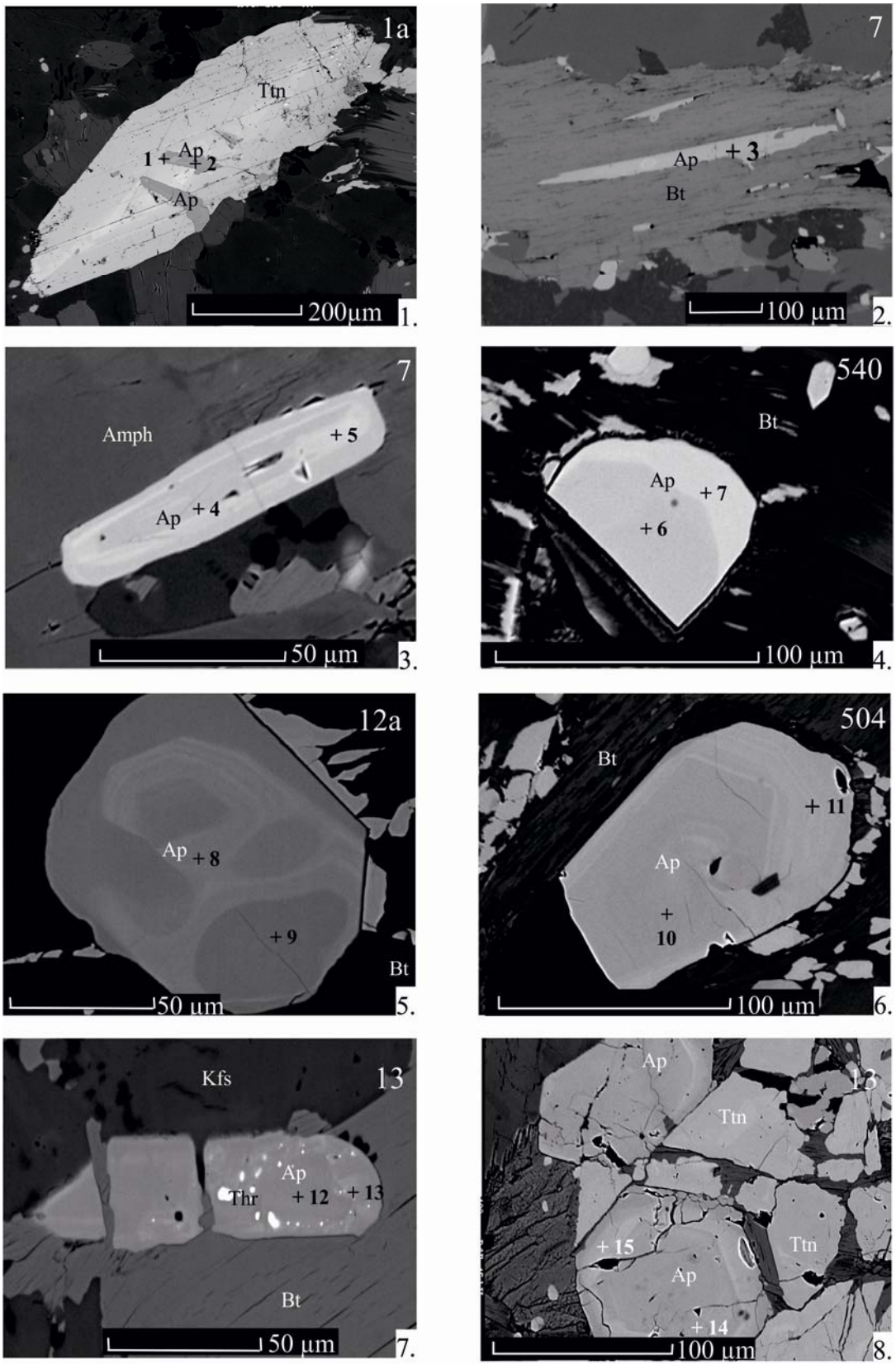

Figure 4. 1. acicular apatite in titanite (enclave); 2. acicular apatite in biotite (enclave); 3. zoned apatite in amphibole (enclave) 4. zoned apatite in biotite (enclave); 5. „Whirlpool" texture of apatite in hybrid rocks; 6. zoned apatite in biotite (granitoid); 7. thorite inclusions in apatite (granitoid); 8. Titanite and zoned apatites (granitoid); (backscattered electron images: numbers on the minerals are place of spot analyses correspond with numbers on the Tab. 3) (Legend: Amph = amphibole; Bt = biotite; Ms = muscovite; Pl = plagioclase; Kfs = K-feldspar; Qz = quartz; Mnz = monazite; Zrn = zircon; Ap = apatite; Ttn = titanite)

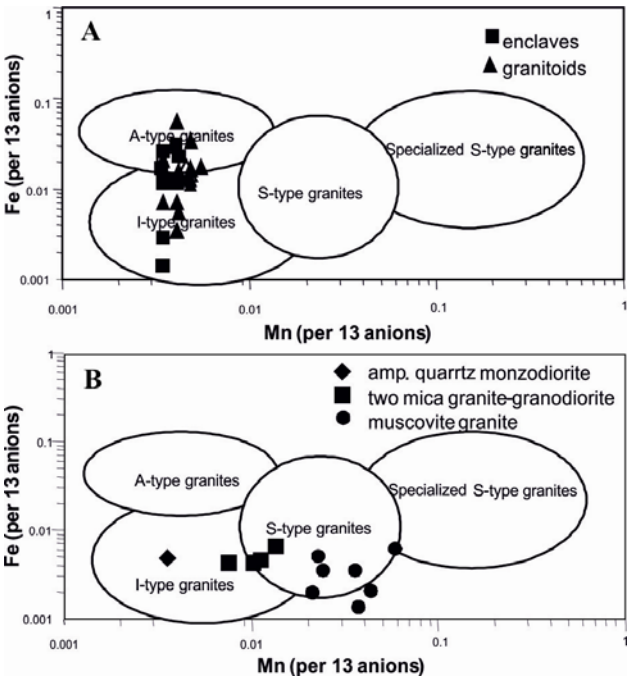

Figure 5. Fe and Mn content of apatite in granitoids Granite fields after Broska et al. (2002); A. Mórágy Subunit.; B. Battona Subunit

monazite and zircon inclusions (Fig. 6/7, 8). It contains a rather high amount of Mn (0.51 wt%). The Mn-content of apatite in quartz and K-feldspar is higher than that of apatite in muscovite. Ce (800 ppm), La, (100 ppm), Nd, Gd, Dy, and Y occur in nearly every apatite in variable amounts (ΣREE≈3600 ppm). Fluorine content is high (3.63 wt%).

5.2.1. Summary

Three types of apatites can be distinguished in the granitoid of Battony Subunit: (1) in amphibole quartz monzodiorite, apatite is acicular, has low Mn content, REE-free, and Fe-bearing; (2) in two-mica granodiorite and granite, apatite is euhedral, stubby, inclusion free, Mn-bearing, with small amounts of Y and REEs, with low Fe, and higher F content; (3) in muscovite granite, apatite is eu- and sub-hedral with inclusions of monacite and zircon, Mn-rich, Y- and REE-bearing, and fluorine rich, with low Fe content (Table 4). The average grain size is 220 μm.

6. DISCUSSION AND CONCLUSION

The ASI of the host magma controls the geochemical properties of apatite (Chu et al., 2011). Apatite which is Mn-free or has low amounts of Mn occurs in metaluminous granitoids (Fig. 5/A, B; Broska et al., 2002). Metaluminous granitoid magma formed at high temperature and consequently at higher oxygen fugacity. The Mn^{2+} is easily oxidized to Mn^{3+}, which can not enter the apatite structure (Belousova et al., 2002). Apatite has a higher Mn concentration in peraluminous granitic magma formed from sedimentary rocks (S-type) at a lower temperature and at reduced conditions (lower oxygen fugacity), and Mn^{2+} substitutes directly for Ca^{2+} in the apatite structure. The Mn content of apatite increases from mafic to felsic rocks (Fig. 5/A, B). The Fe content of apatite is rather variable in metaluminous magmas. The ΣREE content of apatite in I-type granitoids (Mórágy Subunit) basically reflects the different bulk rock ΣREE abundances (e.g. ΣREE=450 ppm in enclaves and in its apatite 4700 ppm; 800 ppm in hybrid rocks and in its apatite 7300 ppm; 270 ppm in granitoids, and in its apatite 3900 ppm).

The LREE concentration of apatite depends on the ASI or D introduced by Montel (1993). Due to the low solubility of monazite in the peraluminous melt (D<1) in the S-type granitoids, REEs, especially Ce and Nd, are concentrated in monazite (Nd_2O_3=10.7–14.00 wt%) and later precipitate apatite depleted in LREEs (Ce=480 ppm, Nd_{max}=850 ppm), whereas in metaluminous rocks (D>1), due to Ca enrichment, Ca is known to destabilize monazite and allanite crystallizes instead of monazite (Montel, 1993; Buda & Nagy, 1995). Due to bulk rock enrichment in REEs, apatite is also enriched in REEs, especially Ce and Nd (Ce=2700 ppm, Nd=850-1400 ppm). Apatite contains lower fluorine (30 600 ppm) and higher chlorine contents (400 ppm) in I-type than in S-type granitoids (F=33 700 ppm, Cl=200 ppm). The low chlorine content of apatite in S-type granitoids is due to the higher solubility of Cl in aqueous solution during the sedimentary processes, according to Sha et al. (1999), and consequently the parental rock of S-type granitoids is depleted in chlorine.

The bulk REE content is rather high in the metaluminous hybrid rocks due to the mixing of different Ca-bearing melts, resulting in enrichment of allanite.

Apatite in metaluminous I-type granitoids is usually acicular or prismatic, zoned (the outer zone is enriched in LREEs) with smaller grain size, and enclosed in titanite, amphibole, biotite, and plagioclase. This crystal habit suggests a faster rate of crystallization and zonation due to active magma where the temperature and composition of melts were more changeable compared with peraluminous melt. Usually it is inclusion-free, but sometimes it contains thorite inclusions. Apatite is stubby, large, and often contains zircon and monazite inclusions without zonation in peraluminous S-type granitoids. Apatite occurs in plagioclase, biotite, muscovite, quartz, and K-feldspar.

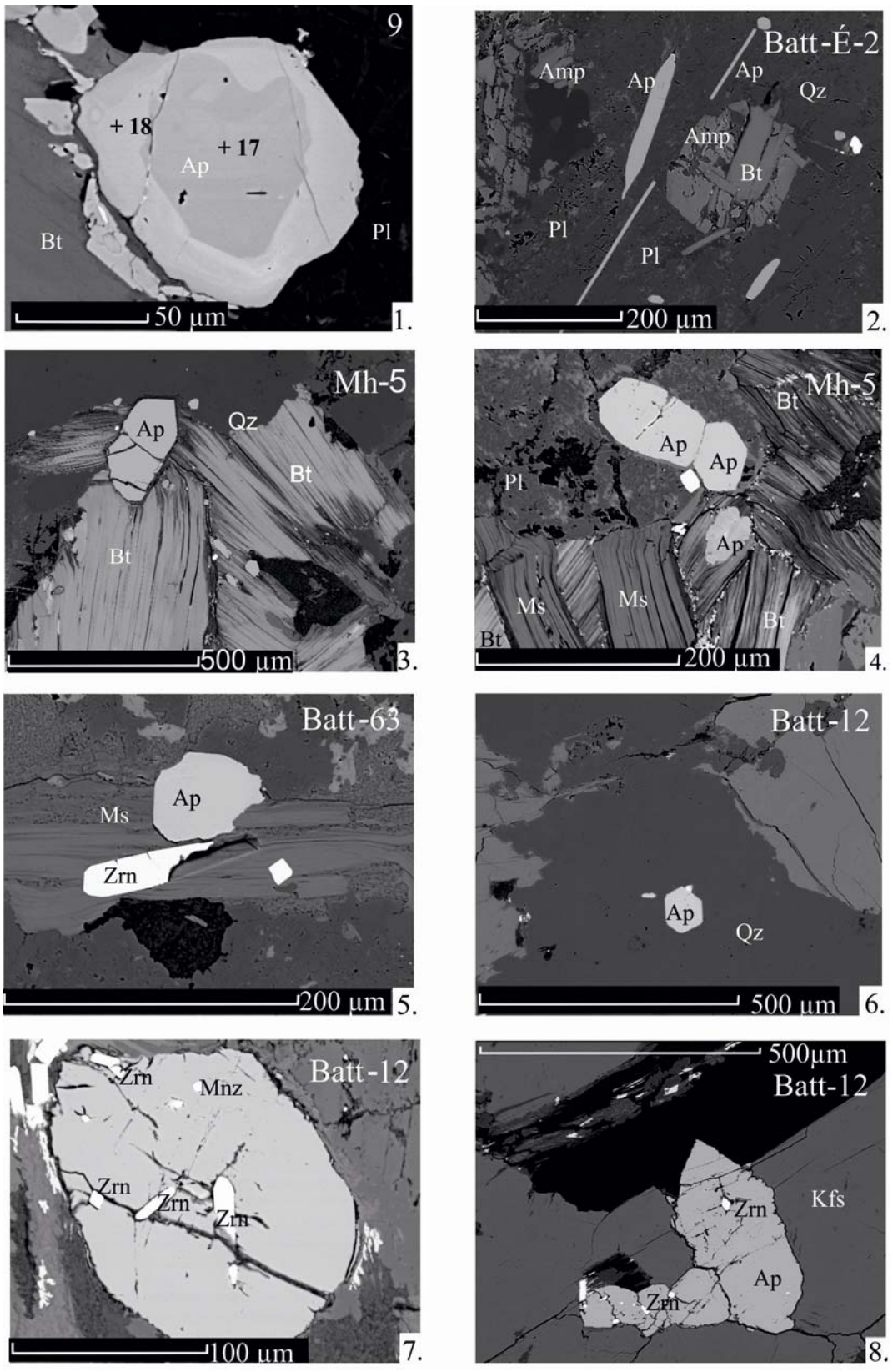

Figure 6. 1. zoned apatit at the border of granite and enclave; 2**.** acicular apatites in amphibole-quartz monzodiorite; 3-4**.** stubby apatites in two mica granitoid; 5–6**.** stubby apatites in muscovite granitoid; 7**.** apatite with zircons and monazites inclusions in muscovite granitoid; 8. Apatite with zircon inclusions in muscovite granitoid (Legend: Amph = amphibole; Bt = biotite; Ms = muscovite; Pl = plagioclase; Kfs = K-feldspar; Qz = quartz; Mnz = monazite; Zrn = zircon; Ap = apatite; Ttn = titanite)

Table 3. Representative chemical composition of apatites from Mórágy Subunit determined by electron microprobe

	Enclaves (monzonite)							Hybrid rock		Granitoid (quartzmonzonite, monzogranite)							Border gr.-encl.	
Sample No.	**1a**		**7**			**540**		**12a**		**504**		**13**				**3**	**9**	
Spot No.	**1**	**2**	**3**	**4**	**5**	**6**	**7**	**8**	**9**	**10**	**11**	**12**	**13**	**14**	**15**	**16**	**17**	**18**
P_2O_5	40.61	41.23	41.28	41.79	41.49	42.12	41.17	41.25	41.72	41.99	41.43	40.94	41.48	41.80	41.05	41.96	42.12	40.91
CaO	54.62	54.54	54.85	55.36	54.44	55.72	54.92	54.72	55.26	55.46	54.66	54.21	54.44	55.80	55.15	55.34	55.33	54.34
F	3.06	2.99	2.68	2.72	2.72	3.18	3.10	3.06	3.09	3.25	3.27	2.97	2.99	3.11	3.62	3.72	3.24	3.11
Cl	0.05	0.03	0.13	0.07	0.08	0.06	0.07	0.08	0.07	0.04	0.00	0.00	0.00	0.00	0.00	0.00	0.07	0.08
SiO_2	0.74	0.45	0.29	0.18	0.52	0.16	0.52	0.41	0.17	0.15	0.39	0.60	0.53	0.21	0.60	0.00	0.19	0.49
Al_2O_3	0.00	0.00	0.00	0.00	0.00	0.00	0.00	0.00	0.00	0.00	0.00	0.00	0.36	0.00	0.00	0.00	0.00	0.00
SrO	0.13	0.16	0.11	0.09	0.10	0.05	0.06	0.07	0.08	0.05	0.05	0.04	0.04	0.00	0.04	0.04	0.08	0.06
FeO	0.04	0.06	0.44	0.30	0.31	0.24	0.33	0.09	0.18	0.14	0.18	0.23	0.82	0.03	0.13	0.15	0.10	0.29
MnO	0.05	0.00	0.06	0.00	0.06	0.05	0.00	0.00	0.00	0.00	0.07	0.07	0.06	0.00	0.00	0.00	0.06	0.05
MgO	0.00	0.00	0.00	0.00	0.00	0.00	0.00	0.00	0.00	0.00	0.00	0.00	0.30	0.00	0.00	0.00	0.00	0.00
Y_2O_3	0.00	0.00	0.00	0.00	0.00	0.00	0.00	0.00	0.00	0.00	0.17	0.31	0.27	0.09	0.35	0.00	0.00	0.00
La_2O_3	0.37	0.23	0.14	0.11	0.34	0.06	0.16	0.26	0.09	0.04	0.10	0.06	0.08	0.03	0.07	0.00	0.11	0.24
Ce_2O_3	0.58	0.39	0.26	0.18	0.63	0.18	0.45	0.57	0.20	0.11	0.29	0.25	0.24	0.17	0.28	0.00	0.25	0.55
Pr_2O_3	0.00	0.00	0.00	0.00	0.00	0.00	0.00	0.00	0.00	0.00	0.00	0.00	0.09	0.00	0.00	0.00	0.00	0.00
Nd_2O_3	0.21	0.13	0.00	0.00	0.21	0.12	0.35	0.14	0.00	0.00	0.24	0.29	0.29	0.13	0.31	0.00	0.11	0.21
Gd_2O_3	0.00	0.00	0.00	0.00	0.00	0.00	0.00	0.00	0.00	0.00	0.10	0.00	0.00	0.00	0.00	0.00	0.00	0.00
O=F, Cl	-1.30	-1.27	-1.16	-1.16	-1.16	-1.35	-1.32	-1.31	-1.32	-1.38	-1.38	-1.25	-1.26	-1.31	-1.52	-1.57	-1.38	-1.33
Ctotal*	99.16	99.00	99.08	99.64	99.74	100.59	99.89	99.34	99.54	99.85	99.57	98.72	100.73	100.06	100.08	99.64	100.28	99.00
	Numbers of ions on the basis of 26 oxygens (F, Cl)																	
P	6.092	6.166	6.164	6.191	6.163	6.196	6.128	6.160	6.196	6.211	6.170	6.130	6.095	6.177	6.106	6.230	6.212	6.140
Si	0.131	0.079	0.051	0.031	0.091	0.028	0.091	0.072	0.030	0.026	0.069	0.106	0.092	0.037	0.105	0.000	0.033	0.087
Al	0.000	0.000	0.000	0.000	0.000	0.000	0.000	0.000	0.000	0.000	0.000	0.000	0.070	0.000	0.000	0.000	0.000	0.000
Ca	10.369	10.322	10.364	10.379	10.233	10.373	10.344	10.341	10.387	10.381	10.302	10.272	10.123	10.436	10.381	10.398	10.327	10.322
Sr	0.013	0.016	0.011	0.009	0.010	0.005	0.006	0.007	0.008	0.005	0.005	0.004	0.004	0.000	0.004	0.004	0.008	0.006
Fe^2	0.006	0.009	0.065	0.044	0.045	0.035	0.049	0.013	0.026	0.020	0.026	0.034	0.119	0.004	0.019	0.022	0.015	0.043
Mn	0.008	0.000	0.009	0.000	0.009	0.007	0.000	0.000	0.000	0.000	0.010	0.010	0.009	0.000	0.000	0.000	0.009	0.008
Mg	0.000	0.000	0.000	0.000	0.000	0.000	0.000	0.000	0.000	0.000	0.000	0.000	0.078	0.000	0.000	0.000	0.000	0.000
Y	0.000	0.000	0.000	0.000	0.000	0.000	0.000	0.000	0.000	0.000	0.020	0.030	0.020	0.010	0.030	0.000	0.000	0.000
La	0.023	0.014	0.009	0.007	0.021	0.004	0.009	0.016	0.006	0.002	0.006	0.004	0.005	0.002	0.004	0.000	0.007	0.015
Ce	0.040	0.030	0.020	0.010	0.040	0.010	0.030	0.040	0.010	0.010	0.020	0.020	0.020	0.010	0.020	0.000	0.020	0.040
Nd	0.010	0.010	0.000	0.000	0.010	0.010	0.020	0.010	0.000	0.000	0.020	0.020	0.020	0.010	0.020	0.000	0.010	0.010
Gd	0.000	0.000	0.000	0.000	0.000	0.000	0.000	0.000	0.000	0.000	0.010	0.000	0.000	0.000	0.000	0.000	0.000	0.000

1. light rim, inclusion in titanite; 2. dark core of same crystal; 3. acicular crystal in biotite; 4. dark part of the crystal; 5. light part of same crystal; 6. dark core; 7. light rim of the crystal; 8-9. "Whirlpool" like light and dark parts in the apatite occurring in hybrid rock; 10. dark core; 11. light rim of the same crystal. 12-13. thorite inclusions in apatite; 14. dark core; 15. light zone in the same crystal; 16. apatite in amphibole; 17. dark core; 18. light rim in the same crystal.* Ctotal = corrected total

Table 4. Representative chemical composition of apatite from Battonya Subunit determined by electron microprobe

	Quartz-monzodiorite					Two-mica granitoid				Muscovite granite						
	1	**2**	**3**	**4**	**5**	**6**	**7**	**8**	**9**	**10**	**11**	**12**	**13**	**14**	**15**	**16**
P_2O_5	41.41	41.78	41.60	41.45	41.96	41.93	42.32	41.64	41.51	42.09	42.32	41.78	41.91	42.11	41.93	42.37
CaO	55.36	55.92	54.96	55.30	55.06	54.93	54.72	54.80	55.15	54.77	54.81	54.86	54.51	54.55	54.77	54.44
F	2.93	2.71	3.67	3.20	2.74	3.41	3.75	3.67	2.92	3.57	3.65	3.51	3.80	3.39	3.75	3.72
Cl	0.00	0.03	0.03	0.04	0.00	0.05	0.05	0.04	0.05	0.00	0.00	0.00	0.00	0.00	0.00	0.00
SiO_2	0.13	0.20	0.12	0.15	0.16	0.07	0.06	0.11	0.07	0.12	0.00	0.09	0.07	0.00	0.00	0.00
Al_2O_3	0.00	0.00	0.00	0.00	0.04	0.00	0.00	0.00	0.00	0.00	0.00	0.00	0.00	0.00	0.00	0.00
Sr_2O	0.09	0.09	0.08	0.10	0.10	0.05	0.06	0.04	0.04	0.04	0.00	0.04	0.05	0.05	0.04	0.04
FeO	0.05	0.10	0.14	0.14	0.07	0.09	0.06	0.06	0.06	0.05	0.05	0.07	0.02	0.03	0.09	0.03
MnO	0.00	0.00	0.00	0.00	0.05	0.20	0.15	0.11	0.16	0.36	0.53	0.33	0.55	0.63	0.87	0.31
MgO	0.00	0.00	0.00	0.00	0.07	0.00	0.00	0.00	0.00	0.00	0.00	0.00	0.00	0.00	0.00	0.00
Y_2O_3	0.00	0.00	0.00	0.00	0.00	0.13	0.18	0.18	0.17	0.23	0.18	0.15	0.19	0.12	0.16	0.17
Ce_2O_3	0.00	0.00	0.00	0.00	0.00	0.09	0.08	0.06	0.07	0.13	0.09	0.08	0.10	0.09	0.10	0.06
Nd_2O_3	0.00	0.00	0.00	0.00	0.00	0.00	0.12	0.00	0.00	0.12	0.00	0.11	0.14	0.12	0.11	0.12
Gd_2O_3	0.00	0.00	0.00	0.00	0.00	0.00	0.00	0.00	0.00	0.10	0.00	0.00	0.00	0.00	0.00	0.00
Dy_2O_3	0.00	0.00	0.00	0.00	0.00	0.10	0.08	0.09	0.00	0.17	0.22	0.16	0.21	0.24	0.31	0.13
O=F,Cl	-1.23	-1.15	-1.55	-1.36	-1.15	-1.45	-1.59	-1.55	-1.24	-1.50	-1.54	-1.48	-1.60	-1.43	-1.58	-1.57
Ctotal*	98.74	99.68	99.05	99.02	99.10	99.60	100.04	99.25	98.96	100.25	100.31	99.75	99.95	99.90	100.55	99.82
Numbers of ions the basis of 26 oxygens (Cl, F)																
P	6.188	6.177	6.215	6.188	6.222	6.227	6.259	6.216	6.196	6.225	6.248	6.211	6.227	6.243	6.209	6.276
Si	0.023	0.035	0.021	0.026	0.028	0.012	0.010	0.019	0.012	0.021	0.000	0.016	0.012	0.000	0.000	0.000
Al	0.000	0.000	0.000	0.000	0.010	0.000	0.000	0.000	0.000	0.000	0.000	0.000	0.000	0.000	0.000	0.000
Ca	10.468	10.463	10.391	10.447	10.332	10.324	10.243	10.353	10.418	10.252	10.241	10.320	10.250	10.234	10.263	10.205
Sr	0.009	0.009	0.008	0.010	0.010	0.005	0.006	0.004	0.004	0.004	0.000	0.004	0.005	0.005	0.004	0.004
Fe^2	0.007	0.015	0.021	0.021	0.010	0.013	0.009	0.009	0.009	0.007	0.007	0.010	0.003	0.004	0.013	0.004
Mn	0.000	0.000	0.000	0.000	0.007	0.030	0.022	0.016	0.024	0.053	0.078	0.049	0.082	0.093	0.129	0.046
Mg	0.000	0.000	0.000	0.000	0.018	0.000	0.000	0.000	0.000	0.000	0.000	0.000	0.000	0.000	0.000	0.000
Y	0.000	0.000	0.000	0.000	0.000	0.010	0.020	0.020	0.020	0.020	0.020	0.010	0.020	0.010	0.010	0.020
Ce	0.000	0.000	0.000	0.000	0.000	0.010	0.010	0.000	0.000	0.010	0.010	0.010	0.010	0.010	0.010	0.000
Nd	0.000	0.000	0.000	0.000	0.000	0.000	0.010	0.000	0.000	0.010	0.000	0.010	0.010	0.010	0.010	0.010
Gd	0.000	0.000	0.000	0.000	0.000	0.000	0.000	0.000	0.000	0.010	0.000	0.000	0.000	0.000	0.000	0.000
Dy	0.000	0.000	0.000	0.000	0.000	0.010	0.000	0.010	0.000	0.010	0.010	0.010	0.010	0.010	0.020	0.010

1-5. Acicular apatite from quartz monzodiorite (Batt. É-2); 6-9. Stubby apatite from two mica granitoid (Mh-5); 10-12. Stubby apatite from muscovite granite (Batt-63); 13-16. Stubby apatite from muscovite granite (Batt.-12).* Ctotal = corrected total

The chemical composition of accessory apatites is related to the ASI of the granitoid host rocks and consequently it is an excellent indicator of the origin of granitoid melts. I-type granitoids, which formed at high temperature under high oxygen fugacity, contain Mn poor, LREE-rich (Ce enrichment is probably also due to oxidation because the ionic radius of Ce^{4+} is close to that of Ca^{2+}; (Fig. 7), chlorine-bearing apatite.

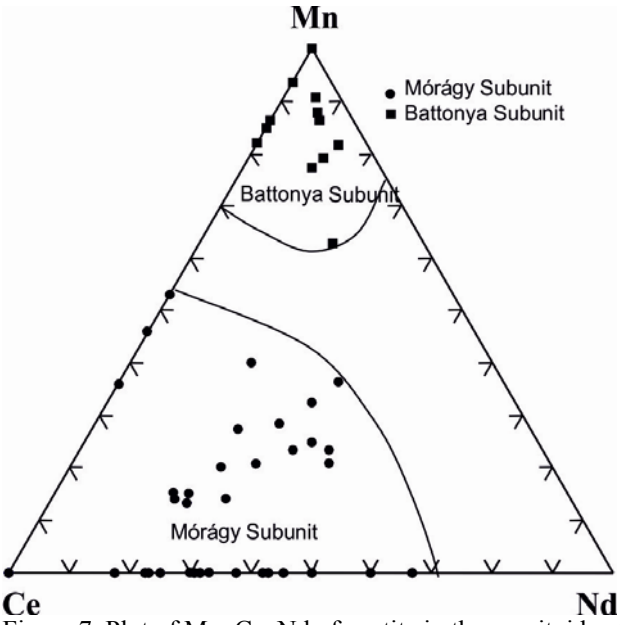

Figure 7. Plot of Mn–Ce–Nd of apatite in the granitoids of two Subunites

S-type granitoids, on the other hand, contain Mn-rich, LREE- and chlorine-depleted apatite due to the reductive low temperature peraluminous melt. It can be concluded from the apatite chemistry that the two occurrences of Variscan granitoids in TMU have different origins. According to these characters the granitoids in Mórágy Subunit are I-type, while in Battonya Subunit it is mainly S-type granitoid that occurs.

ACKNOWLEDGEMENTS

The project was supported by the Hungarian National Research Fund (OTKA), No. K-67787.

REFERENCES

Abdel-Rahman, A.F.M., 1994. *Nature of biotites from alkaline, calc-alkaline and peraluminous magmas.* Journal of Petrology, 35, 525–541.

Ayers, J.C. & Watson, E.B., 1993. *Apatite/fluid partitioning of rare-earth elements and strontium: experimental results at 1.0 GPa and 1000°C and application to models of fluid-rock interaction.* Chemical Geology, 110, 299–314.

Belousova, E.A., Walters, S., Griffin, W.L. & O´Reilly S.Y., 2001.*Trace element signatures of apatites from granitoids of Mount Isa Inlier, north-west Queensland, Australia*. Australian Journal of Earth Sciences, 48, 603–619.

Belousova, E.A, Griffin, W.L., O'Reilly, S.Y. & Fisher N.I., 2002. *Apatite as an indicator mineral exploration: trace-element compositions and their relationship to host rock type*. Journal of Geochemical Exploration, 76, 45–69.

Broska, I., Petrik, I. & Williams, C.T., 2000. *Coexisting monazite and allanite in peraluminous granitoids of the Tribeč Mountains, Western Carpathians*. American Mineralogist, 85, 22–32.

Broska, I., Williams, C.T., Aubin, A. & Uher, P., 2002: *Apatite composition and estimation of fluorine concentration in the West-Carpathian granites.* Geologica Carpathica, 53, spec. issue, 190–192.

Buda, Gy., 1975. *Classification of the Hungarian granitoid rocks on the basis of feldspar investigation.* CBGA Proc. Xth Congress, Sec. III., 67–74.

Buda, Gy. & Nagy, G., 1995. *Some REE-bearing accessory minerals in two types of Variscan granitoids, Hungary.* Geologica Carpathica 46/2, 67–78.

Buda, Gy. & Dobosi, G., 2004. *Lamprophyre-derived high-K mafic enclaves in Variscan granitoids from the Mecsek Mts. (South Hungary).* N. Jb. Mener. Abh., 180/2, 115–147.

Buda, Gy., Koller, F., Kovács, J. & Ulrych, J., 2004. *Compositional variation of biotite from Variscan granitoids in Central Europe: a statistical evaluation.* Acta Mineralogica-Petrographica, 45/1, 21–37.

Buda, Gy., Nagy, G., Pál-Molnár, E. & Koller, F., 2009. *Two main types of Variscan granitoids in Tisia Composite Terrane (Hungary).* Mitt. Österr. Miner. Ges., 155, 39.

Buda, Gy., Koller, F., András, E. & Nagy, G., 2010. *Hungarian Variscan granitoidsand their correlation with surrounding granitoids.* Acta Mineralogica Petrographica Abstract Series, 6, 507.

Chu, M.F., Wang, K.L., Griffin, W.L., Chung, S.L., O'Reilly, S.Y., Pearson, N.J. & Iizuka, Y., 2011. *Apatite composition: tracing petrogenetic processes in Transhimalayan granitoids.* Journal of Petrology, 50/10, 1829–1855.

Csontos, L., 1995. *Tertiary tectonic evolution of the Intra-Carpathian area: a review.* Acta Vulcanologica, 7, 1–13.

Csontos, L. & Vörös, A., 2004. *Mesozoic plate tectonics reconstruction of the Carpathian region.* Paleogeogr. Paleoeco., 210, 1–56.

Debon, F. & Le Fort, P. 1983. *A chemical-mineralogical classification of common plutonic rocks and association.* Transactions of the Royal Society of Edinburgh: Earth and Environmental Science, 73, 135–149.

Haas, J., (ed.) 2001. *Geology of Hungary.* Eötvös University Press, Budapest, 317 p.

Haas, J. & Péró, C., 2004. *Mesozoic evolution of the Tisza Mega-unit.* Int. J. Earth. Sci., 93, 297–313.

Hoshino, M., Kimata, M., Shimizu, M. & Nishida, N., 2007. *Minor-element systematics of fluorapatite and zircon inclusions in allanite-(Ce) from three orogenic felsic rocks: implications for the origin of their host magmas.* The Canadian Mineralogist, 45/6, 1337–1353.

Kovács, S., Hass, J., Buda, Gy., Nagymarosy, A., Szederkényi, T., Árkai, P. & Császár, G., 2000. *Tectonostratigraphic terranes in the pre-Neogen basement of the Hungarian part of the Pannonian area.* Acta Geologica Hungarica, 43/3, 225–328.

Lelkes-Felvári, G., Frank, W. & Schuster, R., 2003. *Geochronological constraints of the Variscan, Permian-Triassic and Eo-alpine (Cretaceous) evolution of the Great Hungarian Plain basement.* Geologica Carpathica, 54/5, 299–315.

Marks, M.A.W., Wenzel, T., Whitehouse, M.J., Loose, M., Zack, T., Barth, M., Worgard, L., Krasz, V., Eby, G.N., Stosnach, H. & Markl, G., 2012. *The volatile inventory (F, Cl, Br, S, C) of magmatic apatite: An integrated analytical approach.* Chemical Geology, 291, 241–255.

Márton, E., 2000. *The Tisza Megatectonic Unit in the light of paleomagnetic data.* Acta Geologica Hungarica, 43/3, 329–343.

Márton, E., 2001. *Tectonic implications of Tertiary paleomagnetic results from the PANCARDI area (Hungarian contribution).* Acta Geologica Hungarica, 44, 135–144.

Montel, J.M., 1993. *A model for monazite/melt equilibrium and application to the generation of granitic magmas.* Chemical Geology,110, 127–146.

Pál-Molnár, E., Kovács, G. & Batki, A., 2001. *Petrographical characteristics of Variscan granitoids of Battonya Unit boreholes (SE Hungary).* Acta Mineralogica-Petrographica, 42, 21–31.

Piccoli, P.M. & Candela, P.A., 2002. *Apatite in Igneous Systems.* Reviews in Mineralogy and Geochemistry, 48/1**,** 255–292.

Sha, L.K. & Chappell, B.W., 1999. *Apatite chemical composition, determined by electron microprobeand laser-ablation inductively coupled plasma massspectrometry, as a probe into granite petrogenesis*. Geochimica et Cosmochimica Acta, 63, 3861–3881.

Schmid, S.M., Bernoulli, D., Fügenschuh, B., Matenco, L., Schefer, S., Schuster, R., Tischler, M. & Ustaszewski, K., 2008. *The Alpine-Carpathian-Dinaridic orogenic system: correlation and evolution of tectonic units.* Swiss Journal of Geosciences,101/1, 139–183.

Received at: 29. 05. 2012
Accepted for publication at: 14. 07. 2012
Published online at; 16. 07. 2012